Earthq Eng & Eng Vib (2012) 11: 403-414 **DOI**: 10.1007/s11803-012-0130-4

# Optimum placement and characteristics of velocity-dependent dampers under seismic excitation

Seyed Amin Mousavi[1†] and Amir K. Ghorbani-Tanha[2‡]

1. *R&D Department, Sabok Sazan Sarie Engineering Company, Tehran, Iran*

2. *School of Civil Engineering, College of Engineering, University of Tehran, Tehran, Iran*

**Abstract:** In this study, through novel drift-based equations of motion in the frequency domain, optimum placement and characteristics of linear velocity-dependent dampers are investigated. In this study, the sum of the square of the absolute values of transfer matrix elements for interstory drifts is considered as the optimization index. Optimum placement and characteristics of dampers are simultaneously obtained by minimizing the optimization index through an incremental procedure. In each step of the procedure, a predefined value is considered as the damper characteristic. The optimum story for this increment is selected such that it leads to a minimum value for the optimization index. The procedure is repeated for the next increments until the optimization index meets its target value, which is obtained according to the desired damping ratio for the overall structure. In other words, the desired overall damping ratio is the input to the proposed procedure, and the optimal placement and characteristics of the dampers are its output. It is observed that the optimal placement of a velocity-dependent damper depends on the damping coefficient of the added damper, frequency of the excitation, and distribution of the mass, stiffness, and inherent damping of the main structure.

**Keywords:** passive control; velocity-dependent damper; optimum placement; optimum damping; transfer matrix; story damping coefficient

## 1 Introduction

With high population growth in cities, developments in construction, and the endless desire of mankind, the need for taller and lighter structures seems to be inevitable. Without protection, these long period and low inherent damping structures would be very vulnerable to dynamic excitations. For these structures, traditional methods such as stiffening and strengthening might be very costly and would probably impose some architectural limitations. Moreover, in the resonance condition of a linear system, the only force that ensures that the system is stable is the damping force. Therefore, additional damping devices, i.e., dampers, can be used as an effective means to reduce the dynamic response of high rise buildings.

Dampers can be divided into three main categories, active, semi-active, and passive dampers. Active dampers are intelligent devices which need a large amount of external energy to operate. Semi-active dampers are intelligent devices but need only a minimal amount of external energy. Passive dampers, however, do not need any external energy. Discussion about the pros and cons of these three types of dampers is out of the scope of this paper; the reader is referred to Soong and Spencer (2002) for an overview and more detailed discussions are available in Soong and Dargush (1997) and Soong (1990). Note that applications of dampers are not limited to any specific structure. However, the main focus of the current study is on high rise buildings.

There are many studies in the literature about optimum design and placement of different kinds of passive dampers. Xia and Hanson (1992) have proposed a simplified method to determine optimum parameters of the added damping and stiffness, ADAS. Through a numerical study, Foti *et al.* (1998) proposed two code-based criteria to evaluate sliding or yielding force of friction or yielding dampers. Recently, a new procedure has been developed by Min *et al*. (2010) to determine the sliding force of a friction damper corresponding to a predefined viscous damping ratio. Modeling seismic excitation as a stationary stochastic process, a sequential procedure based on the degree of controllability concept in the state space has been investigated by Zhang and Soong (1992) to find the optimum characteristics and placement of viscoelastic dampers. This procedure was later modified by Lopez-Garcia (2002) to account for

**Correspondence to**: Seyed Amin Mousavi, No. 4, D.d end Nahid, Hashemiyan St., 3th Neyestan, Pasdaran, Tehran, Iran
Tel: +982122783472; Fax: +982122783492
E-mail: s.a.mousavi@alumni.ut.ac.ir
†Researcher; ‡Assistant Professor

**Supported by**: National Natural Science Foundation of China Under Grant No.50638010 and the Foundation of Ministry of Education for Innovation Group Under Grant No. IRT0518
**Received** December 11, 2011; **Accepted** July 2, 2012

acceleration criteria as well as story drifts. Constantinou and Tadjbakhsh (1983) described a method to evaluate the optimum damping coefficient of the added viscous damper in the first story of a multistory structure. According to their results, there is an extremum point for the damping coefficient which after that, by increasing the damping coefficient, the response of the structure would also increase. Another approach based on the linear quadratic optimal control theory has been proposed by Gluck *et al.* (1996). Adopting the sum of amplitudes of the transfer function as the optimization index, Takewaki (1997) developed a systematic method for finding the optimal damper placement. Unlike Zhang and Soong (1992), Takewaki's procedure is based on the fundamental mode of the structure. Cimellaro and Retamales (2007) compared three different approaches for optimum placement and design of viscous dampers.

In addition to damping distribution, there are several studies which have examined optimal stiffness distribution, such as those carried out by Tsuji and Nakamura (1996) and Connor (2003). There are also some other studies about optimal placement of active dampers which have been briefly described by Soong (1990). The main focus of the present study is on passive dampers. However, some concepts of the optimization techniques proposed for active dampers can also be used for passive dampers, such as those proposed by Masri *et al.* (1981), Pantelides and Cheng (1989), and Agranovich and Ribakov (2010). An effective scheme based on the Genetic Algorithm has been proposed by Apostolakis and Dargush (2010) for optimal distribution of friction dampers and buckling restrained braces. Modeling the seismic excitation by a non-stationary stochastic process, Marano *et al.* (2007) suggested optimal design and placement of linear viscous dampers. Aydin *et al.* (2007) investigated optimal distribution of viscous dampers using the transfer functions amplitude of the base shear.

This brief review includes only some studies in the field of optimization of energy dissipation devices and others in the field of base isolation and vibration absorber are excluded. Moreover, there are many studies devoted to the assessment of damper contribution to different special structures, which are ignored herein due to space limitations.

Note that the optimization index in this study is somewhat a combination between those that have been proposed by Zhang and Soong (1992) and Takewaki (1997). Nevertheless, the derived formulations are very different and the optimization procedure is developed based on a set of target modal damping ratios. The purpose of this study is to address a simple yet accurate scheme to obtain the optimal placement and characteristics of linear velocity-dependent, i.e., linear viscous or viscoelastic, dampers to provide a predefined damping ratio for the overall structure. According to FEMA 450 (2004), structural elements of a building-damper system should be designed to remain elastic for unreduced forces of dampers. In other words, the main objective of damper implementation is to avoid large inelastic deformations in other structural elements. It is true, however, that local nonlinearities are inevitable in severe earthquakes, but the main focus of the present paper is on global response of the structure. Therefore, in this study, only linear-elastic structures are considered.

## 2 Drift-based form of the equations of motion

### 2.1 Drift-based formulation

The governing equations of motion for an $n$ degrees of freedom ($n$-DOFs) linear structure under seismic excitation (Fig. 1) can be written as,

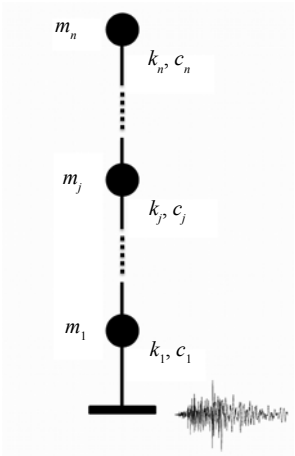


**Fig. 1 *n*-DOF lumped mass model of a shear building**

$$\begin{bmatrix} m_1 & \cdots & 0 \\ \vdots & \ddots & \vdots \\ 0 & \cdots & m_n \end{bmatrix} \ddot{\boldsymbol{u}} + \begin{bmatrix} c_1 + c_2 & \cdots & 0 \\ \vdots & \ddots & \vdots \\ 0 & \cdots & c_n \end{bmatrix} \dot{\boldsymbol{u}} + \begin{bmatrix} k_1 + k_2 & \cdots & 0 \\ \vdots & \ddots & \vdots \\ 0 & \cdots & k_n \end{bmatrix} \boldsymbol{u} = -\begin{pmatrix} m_1 \\ \vdots \\ m_n \end{pmatrix} \ddot{u}_{\mathrm{g}} \tag{1}$$

where $m_j$, $c_j$, and $k_j$ ($j$=1,2,…$n$) denote mass, damping, and stiffness corresponding to the $j$th DOF, respectively; $u$ and $u_{\mathrm{g}}$, respectively, represent horizontal displacement of the structure and ground, and a dot denotes differentiation with respect to time.

If the inherent damping of the system is assumed to be orthogonal, the modal decomposition technique can be used to obtain the solution. Equation (1) can be written in another form which is not as common. For the $j$th DOF, Newton's second law along the lateral direction gives,

$$\sum_{r=j}^{n} m_r \ddot{u}_r + c_j \Delta \dot{u}_j + k_j \Delta u_j = -\ddot{u}_{\mathrm{g}} \sum_{r=j}^{n} m_r \tag{2}$$

where $\Delta u_j$ is the interstory drift of the $j$th floor. Equation (2) can be rewritten in the following form,

$$\sum_{r=j}^{n}\left(m_r\sum_{q=1}^{r}\Delta\ddot{u}_q\right)+c_j\Delta\dot{u}_j+k_j\Delta u_j=-\ddot{u}_{\mathrm{g}}\sum_{r=j}^{n}m_r \quad (3)$$

Assuming that $M$ is the total mass of the structure, dividing Eq. (3) by $M$ gives,

$$\lambda_j\sum_{s=1}^{j-1}\Delta\ddot{u}_s+\sum_{r=j}^{n}\lambda_r\Delta\ddot{u}_r+\frac{c_j}{M}\Delta\dot{u}_j+\frac{k_j}{M}\Delta u_j=-\lambda_j\ddot{u}_{\mathrm{g}} \quad (4)$$

where

$$\lambda_j=\frac{1}{M}\sum_{r=j}^{n}m_r \quad (5)$$

The parameter $\lambda$, called mass index in this study, describes cumulative mass distribution along the height of the building. It can be shown that participation of each story in the seismic input energy depends upon the interstory drift and the mass index of that story. In other words, stories with a lower value for the mass index and interstory drift have less participation in the seismic-induced input energy. Writing Eq. (4) for each story, the drift-based equations of motion can be obtained for the overall building as,

$$\boldsymbol{\Lambda}_1\boldsymbol{\Delta\ddot{u}}+\boldsymbol{C}_{\mathrm{db}}\boldsymbol{\Delta\dot{u}}+\boldsymbol{K}_{\mathrm{db}}\boldsymbol{\Delta u}=-\boldsymbol{\Lambda}_2\ddot{u}_{\mathrm{g}} \quad (6)$$

where

$$\boldsymbol{\Lambda}_1=\begin{bmatrix}\lambda_1 & \lambda_2 & \cdots & \lambda_n\\ \lambda_2 & \lambda_2 & \cdots & \lambda_n\\ \vdots & \vdots & \ddots & \vdots\\ \lambda_n & \lambda_n & \cdots & \lambda_n\end{bmatrix}\ \text{or}\ \Lambda_1(r,s)=\begin{cases}\lambda_s, & \text{for } s\ge r\\ \lambda_r, & \text{for } s<r\end{cases}$$

$$\boldsymbol{\Lambda}_2=\begin{Bmatrix}\lambda_1\\ \lambda_2\\ \vdots\\ \lambda_n\end{Bmatrix},\quad \boldsymbol{C}_{\mathrm{db}}=\frac{1}{M}\begin{bmatrix}c_1 & 0 & \cdots & 0\\ 0 & c_2 & \cdots & 0\\ \vdots & \vdots & \ddots & \vdots\\ 0 & 0 & \cdots & c_n\end{bmatrix},$$

$$\boldsymbol{K}_{\mathrm{db}}=\frac{1}{M}\begin{bmatrix}k_1 & 0 & \cdots & 0\\ 0 & k_2 & \cdots & 0\\ \vdots & \vdots & \ddots & \vdots\\ 0 & 0 & \cdots & k_n\end{bmatrix} \quad (7)$$

Equation (6) can be used to evaluate interstory drift mode shapes and frequencies. It is interesting to note that the modal decomposition technique can be used to solve the above equation, because the mass index and stiffness matrices are positive definite and symmetric.

### 2.2 Damping matrix in the drift based equation

As is clear from Eq. (7), both the damping and stiffness matrices are diagonal. Note that in Eq. (7), it is assumed that damping of each story can be estimated. Nevertheless, it is not practical to assign an appropriate damping coefficient for each individual story. Instead, the damping matrix of a structure should be obtained based on its modal damping ratios (Chopra, 1995).

Many techniques have been proposed to define the damping matrix of a vibrating system, as reported by Adhikari (2000), each of which has its advantages and disadvantages. Among the different alternatives, the proportional damping matrix is the most common technique to construct the damping matrix of a structure. Proportional damping can be divided into four approaches: mass proportional, stiffness proportional, Rayleigh, and Caughey damping. Among these approaches, only stiffness proportional damping can assign a specific value for the damping coefficient of different stories. However, in this approach, only one modal damping ratio, commonly the damping ratio of the first mode, can be considered. This is a great disadvantage of the stiffness proportional technique, because this feature leads to excessive damping in higher modes.

Therefore, according to the current state-of-the-art and state-of-the-practice, it is not possible to determine an appropriate damping coefficient for each individual story in a multistory structure that accounts for all the modal damping ratios.

Both classical and non-classical damping matrices can be used in the drift-based equations. However, they are not necessarily diagonal. Any damping matrix (such as Caughey damping, which is, in general, a full matrix (Bathe, 1996)) can be considered and modified such that it can be used in Eq. (6). In order to do this, a new statement of the drift-based equations is needed. In the earlier subsection, the drift based equations of motion were obtained using Newton's second law. However, these equations can also be obtained directly from Eq. (1). Equation (1) can be rewritten in the following form,

$$\boldsymbol{m}\boldsymbol{T}^{-1}\boldsymbol{T}\ddot{\boldsymbol{u}}+\boldsymbol{c}\boldsymbol{T}^{-1}\boldsymbol{T}\dot{\boldsymbol{u}}+\boldsymbol{k}\boldsymbol{T}^{-1}\boldsymbol{T}\boldsymbol{u}=-\begin{pmatrix}m_1\\ \vdots\\ m_n\end{pmatrix}\ddot{u}_{\mathrm{g}} \quad (8)$$

where

$$\boldsymbol{T}=\begin{bmatrix}1 & 0 & \cdots & 0\\ -1 & 1 & \cdots & 0\\ \vdots & \ddots & \ddots & \vdots\\ 0 & \cdots & -1 & 1\end{bmatrix}\ \text{or}\ T_{rj}=\begin{cases}1, & \text{for } r=j\\ -1, & \text{for } r=j+1\\ 0, & \text{otherwise}\end{cases} \quad (9)$$

Equation (8) can be written as,

$$\boldsymbol{m}\boldsymbol{T}^{-1}\Delta\ddot{\boldsymbol{u}}+\boldsymbol{c}\boldsymbol{T}^{-1}\Delta\dot{\boldsymbol{u}}+\boldsymbol{k}\boldsymbol{T}^{-1}\Delta\boldsymbol{u}=-\begin{pmatrix}m_1\\ \vdots\\ m_n\end{pmatrix}\ddot{u}_{\mathrm{g}} \quad (10)$$

By pre-multiplying Eq. (10) by $\boldsymbol{T}^*$ and dividing the results by the total mass of the structure, $M$, the drift based equation of motion can be obtained as,

$$\frac{1}{M}\boldsymbol{T}^*\boldsymbol{m}\boldsymbol{T}^{-1}\Delta\ddot{\boldsymbol{u}}+\frac{1}{M}\boldsymbol{T}^*\boldsymbol{c}\boldsymbol{T}^{-1}\Delta\dot{\boldsymbol{u}}+\frac{1}{M}\boldsymbol{T}^*\boldsymbol{k}\boldsymbol{T}^{-1}\Delta\boldsymbol{u}=-\frac{1}{M}\boldsymbol{T}^*\begin{pmatrix}m_1\\ \vdots\\ m_n\end{pmatrix}\ddot{\boldsymbol{u}}_{\mathrm{g}} \tag{11}$$

where

$$\boldsymbol{T}^*=\begin{bmatrix}1 & 1 & \cdots & 1\\ 0 & 1 & \cdots & 1\\ \vdots & \ddots & \ddots & \vdots\\ 0 & \cdots & 0 & 1\end{bmatrix} \text{ or } T^*_{rj}=\begin{cases}1\,, & j\geq r\\ 0\,, & \text{otherwise}\end{cases} \tag{12}$$

Note that Eqs. (6) and (11) are the same. However, in Eq. (11), the damping matrix, $\boldsymbol{c}$, can be a full matrix. In other words, Eq. (11) is a generalized form of Eq. (6). As a result, the final form of the drift-based equation of motion can be written as,

$$\boldsymbol{\Lambda}_1\Delta\ddot{\boldsymbol{u}}+\boldsymbol{C}^*_{\mathrm{db}}\Delta\dot{\boldsymbol{u}}+\boldsymbol{K}_{\mathrm{db}}\Delta\boldsymbol{u}=-\boldsymbol{\Lambda}_2\ddot{u}_{\mathrm{g}} \tag{13}$$

where

$$\boldsymbol{C}^*_{\mathrm{db}}=\frac{1}{M}\boldsymbol{T}^*\boldsymbol{c}\boldsymbol{T}^{-1} \tag{14}$$

Note that if additional damping devices are implemented into the structure, the modified damping and stiffness matrix of the drift-based equation would be,

$$\boldsymbol{C}^*_{\mathrm{db}}=\frac{1}{M}\left\{\boldsymbol{T}^*\boldsymbol{c}\boldsymbol{T}^{-1}+\boldsymbol{c}_{\mathrm{d}}\right\},\ \boldsymbol{K}_{\mathrm{db}}=\frac{1}{M}\left\{\boldsymbol{T}^*\boldsymbol{k}\boldsymbol{T}^{-1}+\boldsymbol{k}_{\mathrm{d}}\right\} \tag{15}$$

where $\boldsymbol{c}_{\mathrm{d}}$ and $\boldsymbol{k}_{\mathrm{d}}$ are diagonal matrices of added damping and stiffness such that each diagonal element denotes the added stiffness and damping in its corresponding story.

Transforming Eq. (13) into the frequency domain, the following relation would be obtained,

$$\boldsymbol{A}\,\Delta\boldsymbol{U}(\omega)=-\boldsymbol{\Lambda}_2\ddot{U}_{\mathrm{g}}(\omega) \tag{16}$$

where

$$\boldsymbol{A}=-\omega^2\boldsymbol{\Lambda}_1+\boldsymbol{K}_{\mathrm{db}}+\mathrm{i}\omega\boldsymbol{C}^*_{\mathrm{db}} \tag{17}$$

In Eqs. (16) and (17), i is the imaginary unit, $\Delta\boldsymbol{U}$ and $\ddot{U}_{\mathrm{g}}$ stand, respectively, for Fourier transforms of $\Delta\boldsymbol{u}$ and $\ddot{u}_{\mathrm{g}}$, and $\omega$ indicates circular frequency of the excitation. Equation (16) can be written as

$$\boldsymbol{\Delta U}(\omega)=\boldsymbol{B}(\omega)\,\ddot{U}_{\mathrm{g}}(\omega) \tag{18}$$

where $\boldsymbol{B}(\omega)$ is the transfer matrix given by,

$$\boldsymbol{B}(\omega)=-\boldsymbol{A}^{-1}\boldsymbol{\Lambda}_2 \tag{19}$$

The unit of $\boldsymbol{B}(\omega)$ is square second, $\mathrm{s}^2$.

## 3 Optimal damper placement and characteristics

### 3.1 Minimum transfer matrix criterion

The sum of the square of absolute values of the transfer matrix elements is adopted as the optimization index

$$\mathrm{OI}=\sum_{s=1}^{q}\sum_{j=1}^{n}\left|B_j(\omega_s)\right|^2 \tag{20}$$

where $B_j$ denotes the transfer function of interstory drift of the $j$th floor, i.e., the $j$th element of the vector $\boldsymbol{B}$, defined in Eq. (19), $s$ represents the mode number and $q$ stands for the maximum mode number that has a noticeable contribution on the response of the structure. The optimum story is the one which results in the minimum value for the optimization index. Note that this criterion for the optimal placement is virtually equivalent to considering the sum of the mean square drifts of the building as the optimization index. Because mean square drift of the $j$th story, $\sigma^2_{\mathrm{dj}}$, can be obtained as,

$$\sigma^2_{\mathrm{d}j}=\int_{-\infty}^{\infty}S_{\mathrm{d}j}(\omega)\,\mathrm{d}\omega=\int_{-\infty}^{\infty}\left|B_j(\omega)\right|^2G(\omega)\mathrm{d}\omega \tag{21}$$

where $S_{\mathrm{dj}}$ and $G$, respectively, denote the power spectral density function of the interstory drift of the $j$th story and input base acceleration. As elaborated by Naeim (2001), $G$ depends on the site conditions and shaking intensity of the ground motion. If the base acceleration is assumed to be a white noise, its power spectral density function would be a constant value, $S_0$.

Note that $G$ has an irregular nature and should be smoothed in a mathematical expression. Accordingly, a white noise assumption leads to an ignorable loss of accuracy, due to the fact that variation of the smoothed $G$ is negligible compared to variations of $B$. Some commonly used relations for the smoothed $G$ can be found in Naeim (2001).

It is clear that the square of the absolute value of the transfer function is greatly influenced by its values in the nearby natural frequencies of the structure, such that,

$$\int_{-\infty}^{\infty}\left|B_j(\omega)\right|^2\mathrm{d}\omega\approx\sum_{s=1}^{q}\int_{\omega_s-\Delta\omega}^{\omega_s+\Delta\omega}\left|B_j(\omega)\right|^2\mathrm{d}\omega \tag{22}$$

where $\omega_s$ denotes the natural frequency of the $s$th mode of the structure and $\Delta\omega$ stands for a finite increment in the frequency ordinate. Figure 2 illustrates the validity of this assumption for a 10-story building having a value of 5% as the damping ratio of all modes. Details of the building have been described by Zhang and Soong (1992). For this structure, the sum of the left side of Eq. (22) for all 10 stories is 0.2182. Meanwhile, for example, if the value of $\Delta\omega$ is assumed to be 3, and considering only the first mode, i.e., $q$=1, the sum of the

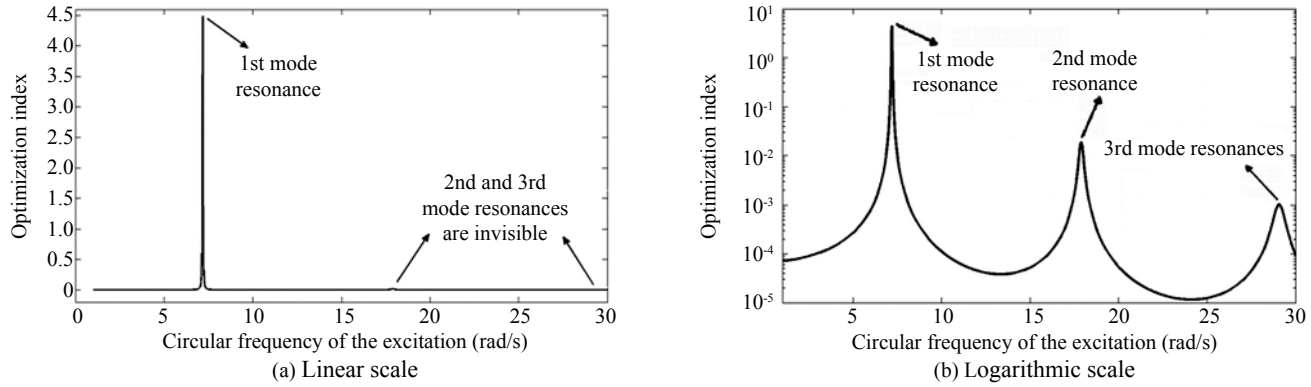


**Fig. 2 Optimization index of the 10-story building for different excitation frequencies**

right side of Eq. (22) for all stories would be 0.2093, i.e., the error is about 4%.

The transfer function in the vicinity of any natural frequency can be represented by a normalized shape function $\psi$ and the value of the transfer function at the fundamental frequency, such that,

$$\left|B_j(\omega)\right|^2 \approx \left|B_j(\omega_s)\right|^2 \psi(\omega) \quad , \quad \omega_s - \Delta\omega < \omega < \omega_s + \Delta\omega \tag{23}$$

The shape function $\psi$, which is similar to a Gaussian function in general, is characterized by mass, stiffness, and damping of the structure. It is interesting to note that the damping of the structure determines the standard deviation of the assumed Gaussian shape function and the stiffness and mass of the structure determine its mean value, i.e., natural frequencies of the structure. It is assumed in the current study that the shape functions of all modes are the same. This assumption is reasonable, according to Fig. 2 (b), and greatly simplifies the optimization procedure.

According to Eqs. (22) and (23) and assuming a white noise base acceleration, Eq. (21) can be simplified to,

$$\sigma_{\mathrm{d}j}^2 \approx S_0 \sum_{s=1}^{q} \Psi_s \left|B_j(\omega_s)\right|^2 \tag{24}$$

where

$$\Psi_s \approx \int_{\omega_s-\Delta\omega}^{\omega_s+\Delta\omega} \psi(\omega)\,\mathrm{d}\omega \tag{25}$$

As is obvious from Eq. (24), the only parameter that can be adjusted by the added dampers to reduce the mean square drift of the $j$th story is the square of the amplitude of $B_j(\omega_s)$. Accordingly, Eq. (20) is considered as the optimization criterion in this study.

### 3.2 Incremental optimization procedure

As stated earlier, an incremental procedure for the optimal damper placement is proposed in this study. In this approach, a predefined increment for the damper characteristic is considered and placed in each story one by one. For an $n$-DOF system, this procedure gives $n$ values for the optimization index. The story which leads to the minimum value for the optimization index would be selected as the optimum story for that increment. This incremental procedure is repeated until the minimum optimization index meets its target value. It is clear that an increment of the damping coefficient for a viscous damper and an increment of both effective damping and stiffness for a viscoelastic damper device should be used. For viscoelastic dampers, the fundamental frequency of the structure should be modified as well. This can be done using the following equation,

$$\left|-\omega^2 \boldsymbol{\Lambda}_1 + \boldsymbol{K}_{\mathrm{db}}\right| = 0 \tag{26}$$

The drift-based equation has two advantages. First, it directly gives the interstory drifts, and second, the stiffness matrix is diagonal, which reduces computational efforts in the case of viscoelastic dampers.

Considering a value of 0.1 MN·s/m as the damping coefficient increment, the optimization indexes are depicted in Fig. 3 for the aforementioned 10-story building. It is clear from Fig. 3 that the optimum placement of the damper completely depends on the frequency of the excitation and it is reasonable to consider only a few of the first lower modes of the structure, for example the first two modes, because optimization indexes of the higher modes are negligible. This assumption greatly simplifies the optimization procedure as mentioned in the preceding subsection.

The incremental procedure should be repeated until the optimization index becomes smaller than its target value. The target optimization index should be evaluated according to the desired modal damping ratios of the overall structure. The proposed incremental procedure is briefly depicted in Fig. 4.

## 4 Examples

The efficiency of the new algorithm is examined through a benchmark 20-story steel moment resistant frame proposed by Spencer *et al.* (2011). The frame is designed according to seismic code specifications for the Los Angeles, California region. In their study,

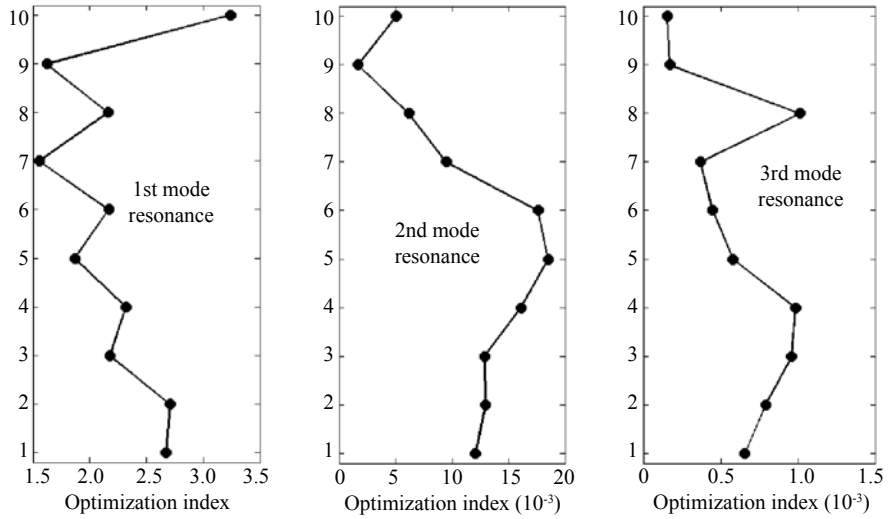


**Fig. 3 Optimization index vs. story level for the first three modes of the 10-story building**

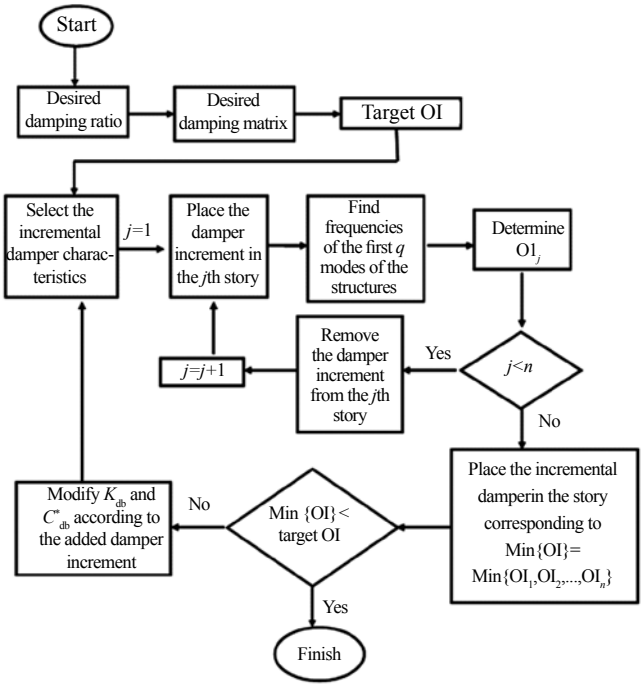


**Fig. 4 Optimization algorithm for velocity-dependent dampers for an *n*-DOF system**

considering 106 active DOFs, the state space model of the structure has been presented. Based on a finite element analysis, however, a shear model of this benchmark with 20 DOFs is obtained and considered in this example. This simplification leads to a minor change in the period of the higher modes. As proposed by Spencer *et al.* (2011), inherent modal damping ratios for different modes are as follows,

$$\xi_j = \min\left\{\frac{\omega_j}{50\omega_1}, 0.1\right\} \tag{27}$$

where $\omega_j$ denotes the natural frequency of the $j$th mode.

The different dynamic characteristics of the model are presented in Tables 1and 2. As suggested by Spencer *et al.* (2011), the N-S components of the following ground motions are considered as the input excitation.

- El Centro 1940, recorded at the Imperial Valley Irrigation District substation in El Centro, California, during the Imperial Valley, California earthquake of May 18, 1940.
- Northridge 1994, recorded at Sylmar County Hospital parking lot in Sylmar, California, during the Northridge, California earthquake of January 17, 1994.
- Hachinohe 1968, recorded at Hachinohe City during the Takochi-oki earthquake of May 16, 1968.
- Kobe 1995, recorded at the Kobe Japanese Meteorological Agency (JMA) station during the Hyogo-ken Nanbu earthquake of January 17, 1995.

The frequency content of these ground accelerations are shown in Fig. 5.

Step 1 Desired damping ratio

Assume that the objective is to increase the modal damping ratios of all modes to 10%.

Step 2 Desired damping matrix

According to the desired modal damping ratios, damping matrix, $\boldsymbol{c}$, is obtained using Caughey damping technique.

Step 3 Target optimization index

After evaluating the desired damping matrix, a value of 0.3532 ($s^4$) is obtained from Eq. (20) as the target optimization index. This value for the uncontrolled structure, i.e., structure with its initial inherent damping, is 8.7486 ($s^4$). For example, if a value of 5% is considered as the damping ratio of all modes, the target optimization index would be 1.4124 ($s^4$). Note that only the first three

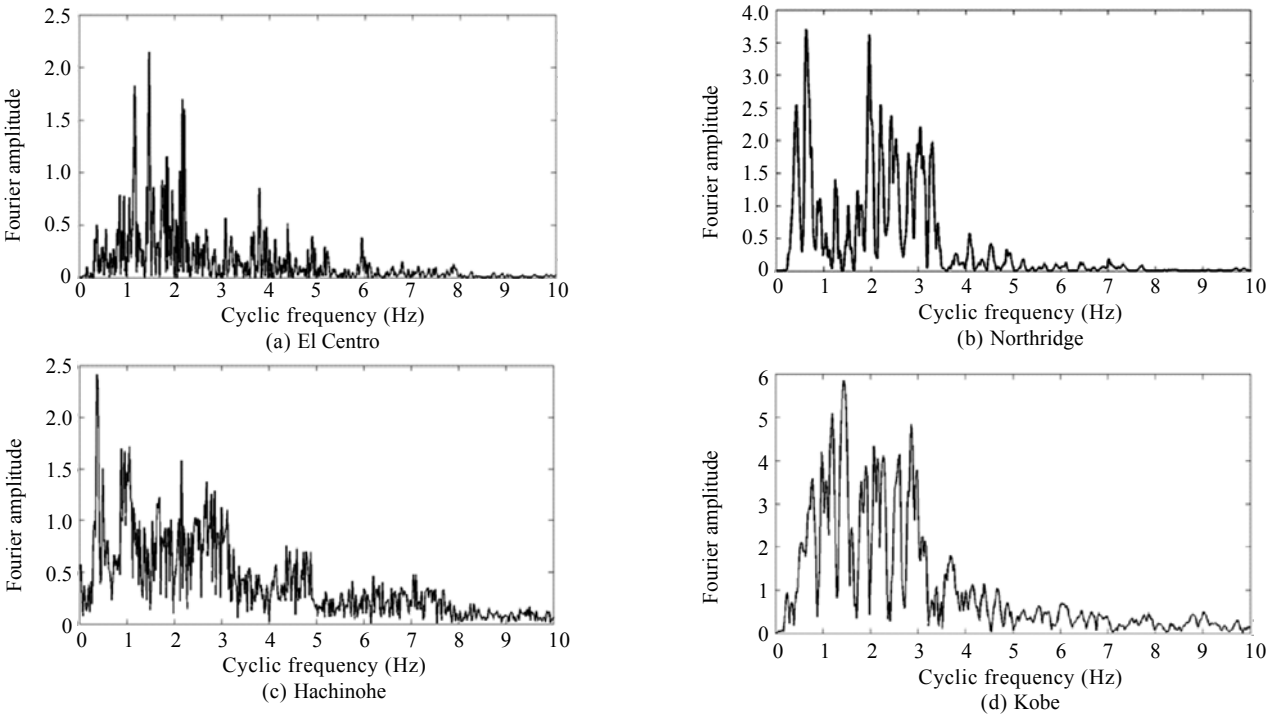


**Fig. 5 Frequency content of input ground accelerations**

**Table 1 Mass and stiffness of the considered model**

| Story | Stiffness (MN/m) | Mass (t) |
|---|---|---|
| 1 | 104.02 | 283 |
| 2 | 136.92 | 276 |
| 3 | 135.94 | 276 |
| 4 | 135.83 | 276 |
| 5 | 134.67 | 276 |
| 6 | 133.38 | 276 |
| 7 | 133.07 | 276 |
| 8 | 132.72 | 276 |
| 9 | 132.31 | 276 |
| 10 | 131.83 | 276 |
| 11 | 125.29 | 276 |
| 12 | 118.13 | 276 |
| 13 | 116.06 | 276 |
| 14 | 108.71 | 276 |
| 15 | 103.37 | 276 |
| 16 | 100.24 | 276 |
| 17 | 91.88 | 276 |
| 18 | 80.68 | 276 |
| 19 | 64.86 | 276 |
| 20 | 45.94 | 276 |

**Table 2 Dynamic characteristics of the considered model**

| Mode | Effective modal mass participation (%) | Period (s) |
|---|---|---|
| 1 | 82.36 | 3.847 |
| 2 | 9.62 | 1.377 |
| 3 | 3.43 | 0.842 |
| 4 | 1.72 | 0.614 |
| 5 | 0.96 | 0.483 |
| 6 | 0.61 | 0.399 |
| 7 | 0.39 | 0.343 |
| 8 | 0.27 | 0.301 |
| 9 | 0.18 | 0.27 |
| 10 | 0.13 | 0.246 |
| 11 | 0.09 | 0.226 |
| 12 | 0.07 | 0.21 |
| 13 | 0.05 | 0.196 |
| 14 | 0.04 | 0.185 |
| 15 | 0.02 | 0.175 |
| 16 | 0.02 | 0.168 |
| 17 | 0.01 | 0.161 |
| 18 | 0.01 | 0.154 |
| 19 | 0.01 | 0.148 |
| 20 | 0 | 0.144 |

modes are considered in this numerical assessment, i.e., $q$=3.

Step 4 Determining characteristics of the incremental damper

In this step, the type of damper is selected. Both solid viscoelastic and viscous dampers are considered in this example. According to FEMA 356 (2000), solid viscoelastic dampers can be modeled using a spring and dashpot in parallel. Therefore, both values for the increment of the effective stiffness and damping coefficient should be selected. Effective damping and stiffness of a viscoelastic damper can be approximated as described in Soong and Dargush (1997),

$$k_{\text{eff}} = \frac{G' A}{t}\kappa \quad , \quad c_{\text{eff}} = \frac{G'' A}{\omega_1 t}\kappa \tag{28}$$

where $G'$ and $G''$ are the shear storage and shear loss modules, respectively; effective area and thickness of the viscoelastic material is denoted by $A$ and $t$, respectively; $\omega_1$ is the fundamental natural frequency of the original structure, and $\kappa$ is a parameter which depends on the damper configuration and its inclination with respect to the horizontal direction. As a result, effective stiffness and damping increments should be selected so that,

$$\frac{\mathrm{d}c}{\mathrm{d}k} = \frac{\eta}{\omega_1} \tag{29}$$

where effective damping and stiffness increments are denoted by d$c$ and d$k$, respectively, and $\eta$ is the loss factor, i.e., ratio of the shear loss modules to the shear storage modules.

Assuming a value of 1.5 for the loss factor, which is a reasonable value as supported by Soong and Dargush (1997), three cases are considered for the damper increment as presented in Table 3. Note that the lower the damper increment, the higher the accuracy of the proposed algorithm.

For a viscous damper, the damping increments are also adopted based on Table 3. It is assumed that viscous dampers introduce no additional stiffness to the structure.

Step 5 Optimization loop

As it is clear from Fig. 4, the optimization loop is made up of inner and outer loops. The inner loop is developed to obtain the optimal placement of the damper increment while the outer loop determines the number of the increments according to the desired level of the modal damping ratios. The results are presented in Tables 4 and 5 for the viscoelastic and viscous dampers, respectively.

The optimization procedure for viscoelastic dampers in Case II is shown in Fig. 6. It is clear that by decreasing the value of the minimum optimization index, the slope

**Table 3 Three damper increments considered in this example**

| | Effective damping increment (MN·s/m) | Effective stiffness increment (MN/m) |
|---|---|---|
| Case I | 10 | 10.89 |
| Case II | 1 | 1.089 |
| Case III | 0.1 | 0.1089 |

**Table 4 Characteristics of the viscoelastic dampers in each story**

| Story | Case I | | Case II | | Case III | |
|---|---|---|---|---|---|---|
| | Effective damping (MN·s/m) | Effective stiffness (MN/m) | Effective damping (MN·s/m) | Effective stiffness (MN/m) | Effective damping (MN·s/m) | Effective stiffness (MN/m) |
| 1 | 30 | 32.67 | 28 | 30.49 | 28 | 30.49 |
| 2 | 20 | 21.78 | 19 | 20.69 | 19.2 | 20.91 |
| 3 | 20 | 21.78 | 19 | 20.69 | 18.6 | 20.26 |
| 4 | 20 | 21.78 | 18 | 19.60 | 17.5 | 19.06 |
| 5 | 20 | 21.78 | 17 | 18.51 | 16.4 | 17.86 |
| 6 | 20 | 21.78 | 15 | 16.34 | 15.1 | 16.44 |
| 7 | 10 | 10.89 | 13 | 14.16 | 13.1 | 14.27 |
| 8 | 10 | 10.89 | 11 | 11.98 | 10.7 | 11.65 |
| 9 | 10 | 10.89 | 8 | 8.71 | 7.8 | 8.49 |
| 10 | 0 | 0 | 4 | 4.36 | 4.3 | 4.68 |
| 11 | 0 | 0 | 3 | 3.27 | 3.3 | 3.59 |
| 12 | 0 | 0 | 2 | 2.18 | 2.2 | 2.40 |
| Other stories | 0 | 0 | 0 | 0 | 0 | 0 |

**Table 5 Damping coefficient of viscous dampers in each story**

| Story | Case I Damping coefficient (MN.s/m) | Case II Damping coefficient (MN.s/m) | Case III Damping coefficient (MN.s/m) |
|---|---|---|---|
| 1 | 40 | 44 | 44.8 |
| 2 | 30 | 29 | 29.6 |
| 3 | 30 | 28 | 28.8 |
| 4 | 20 | 25 | 26.3 |
| 5 | 20 | 13 | 8.8 |
| Other stories | 0 | 0 | 0 |

of the illustrated curve decreases. In other words, it is easy to increase the damping ratio of a vibrating system from zero to 5%, but it is relatively hard to increase its damping ratio from 5% to 10%. This is a well understood concept in structural dynamics, which is again illustrated herein.

According to Tables 4 and 5, the total required damping and stiffness in Case III is the smallest, however it also needs more computational effort. For example, for viscoelastic dampers, Cases I, II, and III, respectively, need 16, 158, and 1563 outer loop iterations. However, with currently available computer software, this is not a critical problem. The maximum displacements and accelerations of the roof for both viscous and viscoelastic dampers are presented in Table 6 for Case III.

It is clear from Table 6 that the displacement responses are more accurately estimated due to the fact that the optimization index has been constructed based on a displacement-based parameter, i.e., square of the interstory drifts. It is interesting to note that the accuracy of the proposed algorithm is higher in the case of the Northridge earthquake because according to the frequency content of this record, which enhances the accuracy of Eq. (22).

Nevertheless, according to Table 6, the proposed technique can accurately increase the damping of the overall structure to a desired level using different velocity-dependent dampers. According to Cimellaro

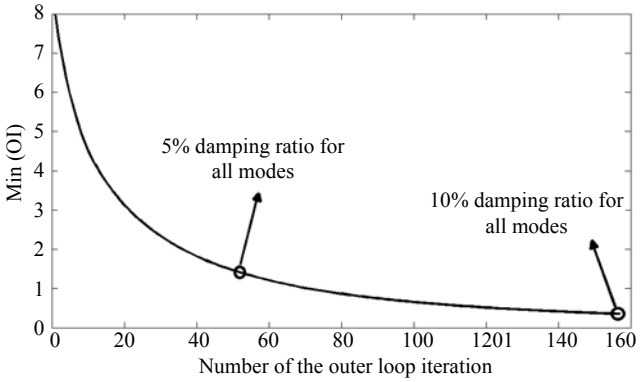


**Fig. 6 Minimum optimization index vs. outer loop iterations**

**Table 6 Different roof response of LA 20-story building using different dampers. (10%=10% damping ratio for all modes, VE=viscoelastic damper, V=viscous damper)**

| | | Maximum displacement (m) | Maximum acceleration (m/s$^2$) |
|---|---|---|---|
| El Centro | 10% | 0.24 | 4.13 |
| | VE | 0.27 | 3.38 |
| | V | 0.26 | 3.23 |
| Northridge | 10% | 0.78 | 10.72 |
| | VE | 0.81 | 11.36 |
| | V | 0.79 | 10.87 |
| Hachinohe | 10% | 0.26 | 2.62 |
| | VE | 0.28 | 2.45 |
| | V | 0.27 | 2.61 |
| Kobe | 10% | 0.45 | 10.15 |
| | VE | 0.45 | 10.28 |
| | V | 0.48 | 10.29 |

and Retamales (2007), if the stiffness of a structure remains constant, the total required damping can roughly be estimated as,

$$C_{\mathrm{A}} = \frac{\left(\xi^{*} - \xi\right) T_0}{\pi} K_0 \tag{30}$$

where $C_{\mathrm{A}}$ is the total required damping, $\xi^{*}$ and $\xi$ indicate, respectively, the desired and initial damping ratio of the fundamental mode, $K_0$ is the total original stiffness of the structure, i.e., the sum of lateral stiffness of all stories, and $T_0$ represents the fundamental period of the structure.

According to Eq. (30), the total required damping in this example is about 222 MN·s/m. However, according to Table 5, this value is 138.3 MN·s/m for Case III. Therefore, the incremental procedure leads to an optimal distribution of dampers according to the target modal damping ratios. To investigate this claim, two patterns of damper distribution are considered with a total value of 138.3 MN·s/m for damping coefficient in both cases: the distribution according to Case III in Table 5, and a uniform distribution of viscous dampers in all stories with damping coefficients of 6.915 MN·s/m. The results are shown in Figs. 7 and 8.

It is clear that the damper distribution proposed in this study is more effective than a uniform distribution, especially in the resonance condition. This fact can also be stated in another language, the language of energy, as shown in Fig. 8. The vertical ordinate in this figure is the transmitted energy into the structure, which is obtained by subtracting the dissipated energy from the input energy. The transmitted energy into the main structure is transformed into kinetic and potential (elastic strain) energies. In other words, the greater the transmitted energy, the greater the response of the structure and probably the greater the damage to the structural and

nonstructural elements. It is obvious that the maximum transmitted energy into the main structure is greater in the case of uniform damper distribution.

Again it should be emphasized that all the dampers in both cases, i.e., Case III and Uniform, have the same damping coefficient and the difference is only in their distribution.

In the LA 20-story building, the mode shape of the interstory drifts for the fundamental mode monotonically decreases from bottom to top. As a result, the optimal places for the dampers are concentrated in the stories with high interstory drifts, which is in agreement with earlier studies. In fact, according to earlier studies, the optimal story for a damper is the story with the highest value for the interstory drift. This is commonly true, however is not general, especially for buildings that have a very light and weak top story. Such light top stories might experience large interstory drifts but

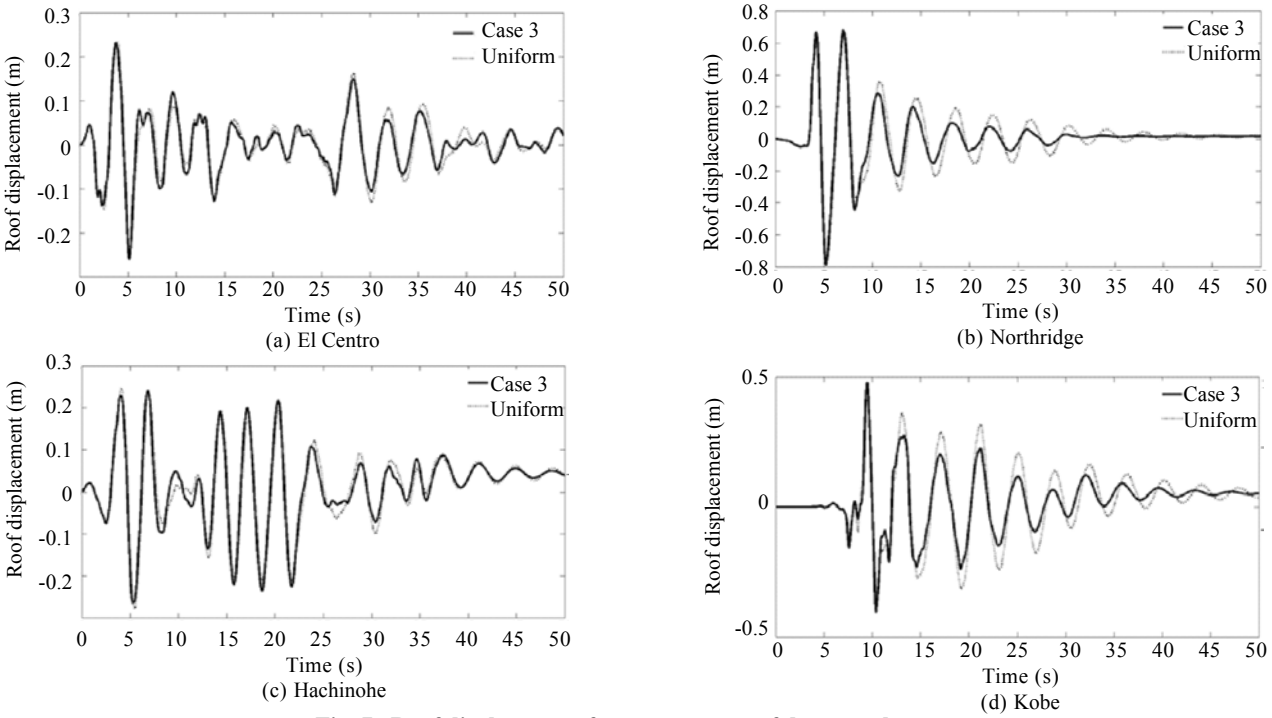


**Fig. 7 Roof displacement for two patterns of damper placement**

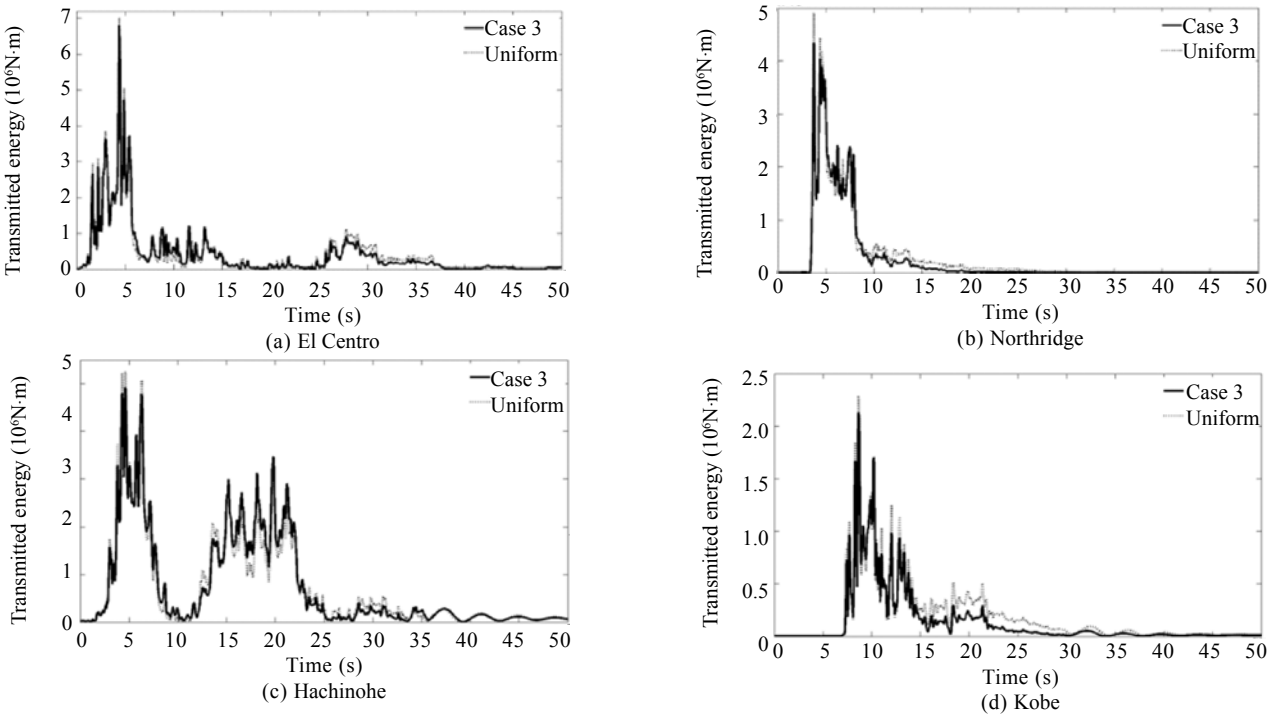


**Fig. 8 Transmitted energy into the structure for two different damper distributions**

they are definitely not appropriate locations for damper placement because they cannot develop a noticeable force into the damper.

## 5 Design considerations

As stated earlier, to use the proposed optimization technique, the desired damping coefficient should be predetermined. There are several schemes to determine this value. However, the authors propose the following procedure.

(1) Analyze and proportion the structure based upon some damping ratios, for example 5% to 20% with 2% increments.

(2) Determine the structural costs for each case, considering damper costs.

(3) Obtain the cost-damping ratio curve from the previous steps.

(4) Select the damping ratio corresponding to the minimum structural cost.

(5) According to the value obtained for the damping ratio and corresponding structural mass and stiffness, obtain the optimum characteristics and placement of the dampers.

The procedure is shown schematically in Fig. 9.

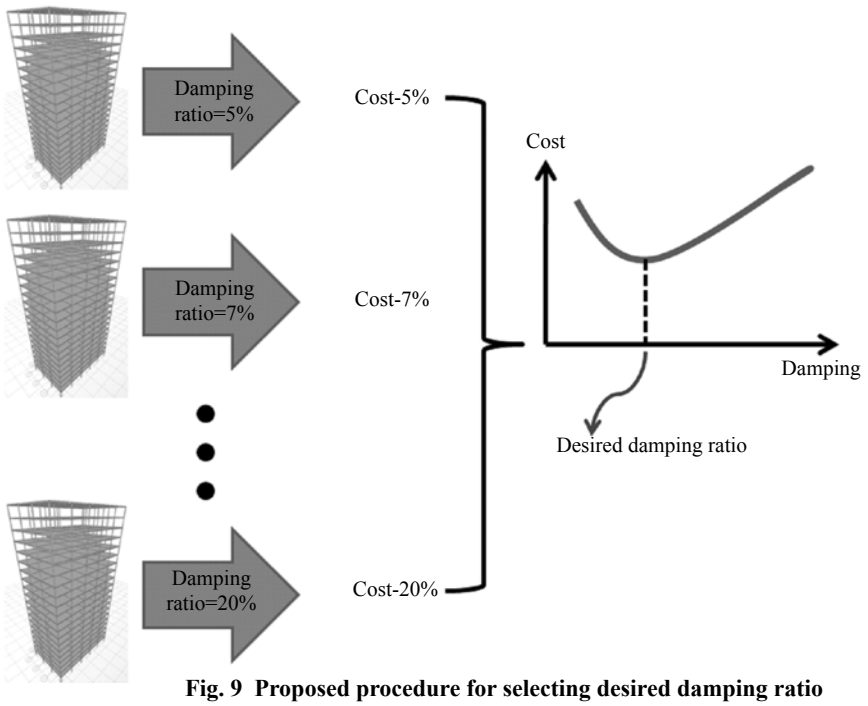


**Fig. 9 Proposed procedure for selecting desired damping ratio**

## 6 Conclusions

A simple yet efficient systematic procedure has been developed during this study to simultaneously find the optimal placement and characteristics of different linear velocity-dependent dampers according to a set of target modal damping ratios. The sum of the square of the absolute value of drift transfer functions for different stories are considered as the optimization index. Using an incremental procedure, the best damper distribution and characteristics are obtained to achieve the smallest value for the optimization index. The proposed optimization algorithm can be used in both classical and non-classical damped systems and its accuracy is adjustable. In other words, by decreasing the damper increment, the accuracy of the proposed algorithm increases. However, very small damper increments need more computational effort.

Note that a drift-based equation of motion has been proposed and developed in the formulation of the optimization algorithm, which leads to a diagonal stiffness matrix. Moreover, if the inherent damping coefficient of each individual story can be estimated, the damping matrix would also be diagonal. The drift-based equation has a full mass matrix, however, this is not a disadvantage because the mass matrix does not change during the proposed algorithm. As a result, having a diagonal stiffness and damping matrix is more valuable than having a diagonal mass matrix. Another advantage of the drift-based equation is that it directly gives the interstory drifts. Modal analysis can be used for this form of equation because modal vectors, i.e., mode shapes of interstory drifts, are orthogonal. During the development of the optimization algorithm, ground acceleration was assumed to be a white noise and it was also assumed that the square of the drifts is dominated by the lower modes of the structure. These two reasonable assumptions greatly simplified the optimization algorithm.

Considering viscous and viscoelastic dampers, the accuracy of the aforementioned assumptions are verified

during a numerical example. It was seen that for seismic excitations which impose more resonance into the fundamental mode of the structure, the accuracy of the proposed algorithm increases.

The main focus of this study was on energy dissipation devices, however, the proposed algorithm can also be modified and used to find the optimal distribution of stiffness along the height of the structure.

## References


Adhikari S (2000), "Damping Models for Structural Vibration," *Dissertation*, Cambridge University, UK.

Agranovich G and Ribakov Y (2010), "A Method for Efficient Placement of Active Dampers in Seismically Excited Structures," *Structural Control and Health Monitoring*, **17**(5): 513–531.

Apostolakis G and Dargush GF (2010), "Optimal Seismic Design of Moment-resisting Steel Frames with Hysteretic Passive Devices," *Earthquake Engineering and Structural Dynamics*, **39**: 355–376.

Aydin E, Boduroglu MH and Guney D (2007), "Optimal Damper Distribution for Seismic Rehabilitation of Planar Building Structures," *Engineering Structures*, **29**(2):176–185.

Bathe KJ (1996), *Finite Element Procedures*, Prentice Hall, Upper Saddle River, NJ.

Chopra AK (1995), *Dynamics of Structures. Theory and Applications to Earthquake Engineering*, Prentice hall, Englewood Cliffs, NJ.

Cimellaro GP and Retamales R (2007), "Optimal Softening and Damping Design for Buildings," *Structural Control and Health Monitoring,* **14**: 831–857.

Connor JJ (2003), *Introduction to Structural Motion Control*, Prentice Hall, Upper Saddle River.

Constantinou MC and Tadjbakhsh IG (1983), "Optimum Design of a First Story Damping System," *Computers & Structures,* **17**(2): 305–310.

FEMA (2000), *Prestandard and Commentary for the Seismic Rehabilitation of Buildings (FEMA 356),* Federal Emergency Management Agency, Washington, DC.

FEMA (2004), *NEHRP Recommendation Provisions for Seismic Regulations for New Buildings and Other Structures* (*FEMA 450*), Federal Emergency Management Agency, Washington, DC.

Foti D, Bozzo L and Lopez-Almansa F (1998), "Numerical Efficiency Assessment of Energy Dissipators for Seismic Protection of Buildings," *Earthquake Engineering and Structural Dynamics*, **27**: 543–556.

Gluck N, Reinhorn AM, and Levy R (1996), "Design of Supplemental Dampers for Control of Structures," *ASCE Journal of Structural Engineering*, **122**(12): 1394–1399.

Lopez-Garcia D (2002), "Efficiency of a Simple Approach to Damper Allocation in MDOF Structures," *Journal of Structural Control*, **9**: 19–30.

Marano GC, Trentadue F and Greco R (2007), "Stochastic Optimum Design Criterion of Added Viscous Dampers for Buildings Seismic Protection," *Structural Engineering and Mechanics*, **25**(1): 21–37.

Masri SF, Bekey GA and Caughey TK (1981), "Optimum Pulse Control of Flexible Structures," *Journal of Applied Mechanics,* **48**: 619–626.

Min KW, Seong JY and Kim J (2010), "Simple Design Procedure of a Friction Damper for Reducing Seismic Responses of a Single-story Structure," *Engineering Structures*, **32**: 3539–3547.

Naeim F(2001), *The Seismic Design Handbook,* 2nd ed, Springer-Verlag, New York.

Pantelides CP and Cheng FY (1989), "Optimal Location of Active Controllers Subjected to Seismic Excitations," *Computer Utilization in Structural Engineering*, ASCE, pp. 110–120.

Soong TT (1990), *Active Structural Control: Theory and Practice*, John Wiley & Sons, New York, NY.

Soong TT and Dargush GF (1997), *Passive Energy Dissipation Systems in Structural Engineering*, John Wiley, Chichester, UK.

Soong TT and Spencer BF (2002), "Supplemental Energy Dissipation: State-of-the-art and State-of-the-practice," *Engineering Structures*, **24**: 243–259.

Spencer BF, Christenson RE and Dyke SJ (2011), "Next Generation Benchmark Control Problem for Seismically Excited Buildings," http://sstl.cee.illinois.edu, March 2011.

Takewaki I (1997), "Optimal Damper Placement for Minimum Transfer Functions," *Earthquake Engineering and Structural Dynamics,* **26**: 1113–1124.

Tsuji M and Nakamura T (1996), "Optimum Viscous Dampers for Stiffness Design of Shear Buildings," *The Structural Design of Tall Buildings,* **5**: 217-234.

Xia C and Hanson RD (1992), "Influence of ADAS Element Parameters on Building Seismic Response," *ASCE Journal of Structural Engineering,* **118**(7): 1903–1918.

Zhang RH and Soong TT (1992), "Seismic Design of Vescoelastic Dampers for Structural Applications," *ASCE Journal of Structural Engineering*, **118**(5): 1375–1392.